Input-output theory of cavities in the ultra-strong coupling regime: the case of a time-independent vacuum Rabi frequency

Cristiano Ciuti[1,*] and Iacopo Carusotto[2]

[1] *Laboratoire Pierre Aigrain, Ecole Normale Supérieure, 24, rue Lhomond, 75005 Paris, France*
[2] *BEC-CNR-INFM and Dipartimento di Fisica, Università di Trento, I-38050 Povo, Italy*

(Dated: February 6, 2008)

We present a full quantum theory for the dissipative dynamics of an optical cavity in the ultra-strong light-matter coupling regime, in which the vacuum Rabi frequency is a significant fraction of the active electronic transition frequency and the anti-resonant terms of the light-matter coupling play an important role. In particular, our model can be applied to the case of intersubband transitions in doped semiconductor quantum wells embedded in a microcavity. The coupling of the intracavity photonic mode and of the electronic polarization to the external, frequency-dependent, dissipation baths is taken into account by means of quantum Langevin equations in the input-output formalism. In the case of a time-independent vacuum Rabi frequency, exact analytical expressions for the operators are obtained, which allows us to characterize the quantum dissipative response of the cavity to an arbitrary initial condition (vacuum, coherent field, thermal excitation). For a vacuum input in both the photonic and electronic polarization modes, the ground state of the cavity system is a two-mode squeezed vacuum state with a finite population in both photonic and electronic modes. These excitations are however virtual and can not escape from the cavity: for a vacuum input, a vacuum output is found, without any trace of the intracavity squeezing. For a coherent photonic input the linear optical response spectra (reflectivity, absorption, transmission) have been studied, and signatures of the ultra-strong coupling have been identified in the asymmetric and peculiar anticrossing of the polaritonic eigenmodes. Finally, we have calculated the electroluminescence spectra in the case of an incoherent electronic input: the emission intensity in the ultra-strong coupling regime results significantly enhanced as compared to the case of an isolated quantum well without a surrounding cavity.

In recent years, the study of cavity quantum electrodynamics[1,2] has been a subject of an intense and fruitful research. In particular, a considerable deal of activity has been devoted to the so-called strong light-matter coupling regime. This regime is achieved when the vacuum Rabi frequency Ω_R of an electronic excitation (i.e., the Rabi frequency associated to electric field vacuum fluctuations) exceeds the frequency broadening of the photonic and electronic excitations. In the case of atoms in high-finesse cavities (either in the optical[1] or in the microwave[2] domains), the strong coupling occurs thanks to the strong spatial localization of the electromagnetic field and the very high quality factors (as high as 10^8) of the cavity mode and the atomic resonance, but the vacuum Rabi frequency Ω_R still remains a tiny fraction of the active transition frequency ω_{eg}. In the case of semiconductor planar microcavities[3,4], the quality factors are by far less impressive (typically not much larger than $Q \approx 10^3$), but the strong coupling can be still comfortably obtained thanks to the strong photon confinement and the large electric dipole moment of the active electronic transitions in the quantum well. Both these facts cooperate to give a much larger vacuum Rabi frequency. Using inter-subband transitions in doped semiconductor quantum wells[4,5,6,7,8], it is even possible to achieve an unprecedented ultra-strong light-matter coupling regime[9], in which the vacuum Rabi frequency Ω_R becomes comparable to the intersubband electronic transition ω_{12}. In this regime, the standard rotating wave approximation is no longer valid, and anti-resonant terms of the light-matter interaction start playing a significant role. In particular, it has been shown in Ref.9 that the ground state of an isolated cavity is a two-mode squeezed vacuum containing a finite number of virtual and correlated photons and intersubband excitations.

In the present paper, a full quantum description of the system is developed, which now explicitely includes the coupling to dissipation baths. In the specific case of intersubband excitations in planar semiconductor microcavities considered here, the dissipation baths are not only responsible for damping rates which are typically as large as 5-10 % of the transition frequency[4,7,8], but also provide the way of exciting and observing the cavity dynamics. The photonic mode is coupled to external world mostly because of the finite reflectivity of the cavity mirrors, while the intersubband transition is coupled to other excitations in the semiconductor material, e.g. acoustic and optical phonons, and free carriers in levels other than the ones involved in the considered transition. In particular, the coupling to this electronic bath allows one to electrically excite the intersubband transitions.

The theory here developed is based on the so-called input-output formalism[10,11,12], in which the dynamics of the electronic polarization and cavity photonic fields is described in terms of quantum Langevin equations for the two coupled quantum fields. Differently from previous treatments, we have to take into account here all the anti-resonant terms of the vacuum Rabi coupling, which forces us for consistency to keep track in an exact way of the frequency dependence of the dissipation baths.

The paper is organized as follows. In Sec. I, we introduce the model Hamiltonian for the considered system and for the baths. In Sec. II, the quantum Langevin equations for the intracavity photonic and electronic polarization fields are derived. Their exact solution for the intracavity operators as well as for the output operators is given in Sec.III. The case of a vacuum input both for the photonic and polarization fields is analyzed in Sec. IV, where the properties of the ground state of the system are characterized and the presence of squeezing in the intra-cavity fields is pointed out. The question of the observability or not of this squeezing in the output field is addressed in Sec. V, where we predict that no squeezing can be observed in the output modes unless the input is itself squeezed.

After the brief discussion of single- and double-sided cavities of Sec.VI A, the main features of the linear optical spectra (reflectivity, absorption, transmission) under optical excitation are considered in Sec.VI B. The electroluminescence emission spectra under an electronic excitation are studied in Sec.VI C, where a remarkable enhancement of the emission intensity is found as compared to the case of an isolated quantum well in free space. Conclusions and perspectives are finally drawn in Sec. VII.

I. MODEL HAMILTONIAN

As schematically shown in Fig.1, the Hamiltonian of the present system contains three main blocks:

$$H = H_{sys} + H_{bath}^{phot} + H_{bath}^{el} \ , \tag{1}$$

where H_{sys} is the Hamiltonian describing the closed cavity system, while H_{bath}^{phot} and H_{bath}^{el} take into account the coupling to respectively the photonic and electronic reservoirs.

The Hamiltonian $H_{sys} = H_0 + H_{res} + H_{anti}$ for the closed cavity system has the typical Hopfield[13] form already discussed in detail in Ref. 9, and contains three parts respectively describing the energy of the bare cavity photons and of the electronic excitations (H_0), the resonant part of the light-matter interaction (H_{res}), and the anti-resonant terms[34] usually neglected in the so-called rotating-wave approximation[20] (H_{anti}):

$$H_0 = \sum_{\boldsymbol{k}} \hbar\omega_{\mathrm{cav},k} \left(a_{\boldsymbol{k}}^\dagger a_{\boldsymbol{k}} + \frac{1}{2} \right) + \sum_{\boldsymbol{k}} \hbar\omega_{12} \ b_{\boldsymbol{k}}^\dagger b_{\boldsymbol{k}} \ , \tag{2}$$

$$H_{res} = \hbar \sum_{\boldsymbol{k}} \{ i\Omega_{R,k} (a_{\boldsymbol{k}}^\dagger b_{\boldsymbol{k}} - a_{\boldsymbol{k}} b_{\boldsymbol{k}}^\dagger) + D_k (a_{\boldsymbol{k}}^\dagger a_{\boldsymbol{k}} + a_{\boldsymbol{k}} a_{\boldsymbol{k}}^\dagger) \} \ , \tag{3}$$

$$H_{anti} = \hbar \sum_{\boldsymbol{k}} \{ i\Omega_{R,k} (a_{\boldsymbol{k}} b_{-\boldsymbol{k}} - a_{\boldsymbol{k}}^\dagger b_{-\boldsymbol{k}}^\dagger) + D_k (a_{\boldsymbol{k}} a_{-\boldsymbol{k}} + a_{\boldsymbol{k}}^\dagger a_{-\boldsymbol{k}}^\dagger) \} \ . \tag{4}$$

Translational invariance along the cavity plane has been here assumed. $a_{\mathbf{k}}^\dagger$ is the creation operator of a cavity photon with in-plane wave-vector $\mathbf{k}$ and energy $\hbar\omega_{\mathrm{cav},\mathbf{k}}$. $b_{\mathbf{k}}^\dagger$ is the creation operator of the *bright* intersubband excitation mode of wavevector $\mathbf{k}$ of the doped quantum well[9]:

$$b_{\mathbf{k}}^\dagger = \frac{1}{\sqrt{N_{QW}\, \sigma_{el}\, S}} \sum_{j=1}^{N_{QW}} \sum_{|\mathbf{q}|<k_F} c_{2,\mathbf{q}+\mathbf{k}}^{(j)\dagger} \, c_{1,\mathbf{q}}^{(j)}. \tag{5}$$

Here, N_{QW} is the number of quantum wells present in the cavity (which are assumed for simplicity to be situated at the antinodes of the cavity mode, and therefore identically coupled to the photonic mode), $\sigma_{el} = N_{el}/S$ is electron density per unit area in each quantum well and S is the quantization area. The fermionic operator $c_{1,\mathbf{q}}^{(j)}$ annihilates an electron of in-plane wavevector $\mathbf{q}$ from the lowest subband of the j-th quantum well, while $c_{2,\mathbf{q}}^{(j)\,\dagger}$ creates an electron with wavevector $\mathbf{q}$ in the second, excited, subband of the j-th quantum well. k_F is the Fermi wavevector of the two-dimensional electron gas in each well, and the electronic ground state is written as:

$$|F\rangle = \prod_{j=1}^{N_{QW}} \prod_{|\mathbf{q}|<k_F} c_{1,\mathbf{q}}^{(j)\,\dagger} \, |0_{cond}\rangle \tag{6}$$

in terms of the empty conduction band state $|0_{cond}\rangle$. In the following, we shall always restrict ourselves to a weak excitation regime:

$$\frac{1}{S} \sum_{\mathbf{k}} \langle b_{\mathbf{k}}^\dagger \, b_{\mathbf{k}} \rangle \ll \sigma_{el}, \tag{7}$$

in which the operators $b_{\mathbf{k}}$ are approximately bosonic:

$$\left[b_{\mathbf{k}}, b^{\dagger}_{\mathbf{k}'}\right] = \delta_{\mathbf{k},\mathbf{k}'}. \tag{8}$$

The $N_{QW}N_{el}-1$ states orthogonal to $b^{\dagger}_{\mathbf{k}}|F\rangle$ are dark excitations (uncoupled to the cavity photon) which do not play any role in the optical processes taking place in the system. The first and second electronic subbands have been here assumed to be perfectly parallel[23], with a momentum-independent transition frequency ω_{12}.

$\Omega_{R,k}$ is the vacuum Rabi frequency which quantifies the strength of the light-matter dipole coupling: in the case of intersubband transitions in doped quantum wells[9], it can become a significant fraction of the intersubband transition ω_{12}. The explicit expression is

$$\Omega_{R,k} = \left(\frac{2\pi e^2}{\epsilon_{\infty} m_0 L^{\mathrm{eff}}_{\mathrm{cav}}} \, \sigma_{el} \; N_{QW} \; f_{12} \sin^2\theta \right)^{1/2} , \tag{9}$$

where $L^{\mathrm{eff}}_{\mathrm{cav}}$ is the effective length of the cavity mode and θ is the intracavity photon propagation angle such that $\sin\theta = ck/(\omega_{12}\sqrt{\epsilon_{QW}})$.

D_k is the related term originating from the squared electromagnetic vector potential term in the minimal coupling light-matter Hamiltonian[9]: for a typical quantum well potential, one has $D_k \simeq \Omega^2_{R,k}/\omega_{12}$.

The environment of the open cavity system is modeled by two baths of excitations, associated to respectively the photonic and the electronic degrees of freedom. In this paper, we shall focus our attention on cavity configurations in which the photonic mode is coupled to the external electromagnetic field via the finite transmittivity of the planar mirrors enclosing the cavity, as recently done[4,5,7]. In a planar geometry, the coupling of the cavity photon to the extra-cavity electromagnetic modes is well described by the Hamiltonian:

$$H^{ph}_{bath} = \int dq \sum_{\mathbf{k}} \hbar\omega^{ph}_{q,\mathbf{k}} \left(\alpha^{\dagger}_{q,\mathbf{k}} \alpha_{q,\mathbf{k}} + \frac{1}{2} \right) + i\hbar \int dq \sum_{\mathbf{k}} \left(\kappa^{ph}_{q,\mathbf{k}} \, \alpha_{q,\mathbf{k}} \; a^{\dagger}_{\mathbf{k}} - \kappa^{ph\,*}_{q,\mathbf{k}} \, \alpha^{\dagger}_{q,\mathbf{k}} a_{\mathbf{k}} \right) , \tag{10}$$

where $\omega^{ph}_{q,\mathbf{k}}$ is the frequency of an extra-cavity photon with in-plane wavevector $\mathbf{k}$ and wavevector q in the orthogonal direction and $\alpha^{\dagger}_{q,\mathbf{k}}$ is the corresponding creation operator, obeying the commutation rule $[\alpha_{q,\mathbf{k}}, \alpha^{\dagger}_{q',\mathbf{k}'}] = \delta(q-q')\delta_{\mathbf{k},\mathbf{k}'}$. The coupling between the cavity and the extracavity radiation fields is quantified by the tunneling matrix element $\kappa^{ph}_{q,\mathbf{k}}$ through the cavity mirror, whose value depends on the specific mirror structure and can be calculated by solving the classical Maxwell equations.

The Hamiltonian (10) takes into account a single radiative bath, coupled to the cavity through one of its mirrors. For the sake of simplicity, we shall start our analysis from this simplified case, which is then extended in Sec.VI A to the more realistic case of two photonic baths coupled to the cavity through the front and the back mirrors. All this discussion is performed by neglecting the anti-resonant terms in H^{phot}_{bath} whose effect is quantitatively small; the general case including would not however pose any additional problem, and is considered and solved in Appendix A.

Concerning the bath coupled to the electronic transition, the modelling is not as straightforward as in the photonic case. In the case of intersubband transitions in doped semiconductor quantum wells[14,15], the damping and decoherence of the electronic transition at the frequency ω_{12} is due to the interplay of different processes, such as the interaction with crystal phonons (optical and acoustical), the scattering with impurities and with free carriers in levels other from the ones involved in the considered electronic transition[16]. As our purpose is to study the role of the electronic losses and decoherence on the peculiar quantum optical properties of cavities in the ultra-strong coupling regime, we do not attempt here to address the specific nature of the decoherence channels, but we will rather model them as a phenomenological bath of harmonic excitations in the spirit of the Caldeira-Leggett model[17]. As for the photonic bath, the harmonic oscillators modes coupled to the intersubband excitation of wavevector $\mathbf{k}$ are labelled by a continuous index q and have frequency $\omega^{el}_{q,\mathbf{k}}$. They affect the electronic intersubband transition according to the Hamiltonian:

$$H^{el}_{bath} = \int dq \sum_{\mathbf{k}} \hbar\omega^{el}_{q,\mathbf{k}} \left(\beta^{\dagger}_{q,\mathbf{k}} \beta_{q,\mathbf{k}} + \frac{1}{2} \right) + i\hbar \int dq \sum_{\mathbf{k}} \left[\kappa^{el}_{q,\mathbf{k}} \, \beta_{q,\mathbf{k}} \; b^{\dagger}_{\mathbf{k}} - \kappa^{el\,*}_{q,\mathbf{k}} \, \beta^{\dagger}_{q,\mathbf{k}} b_{\mathbf{k}} \right] .$$

Here, the bath operators $\beta_{q,\mathbf{k}}$ satisfy the harmonic oscillator commutation rule $[\beta_{q,\mathbf{k}}, \beta^{\dagger}_{q',\mathbf{k}'}] = \delta(q-q')\delta_{\mathbf{k},\mathbf{k}'}$. $\kappa^{el}_{q,\mathbf{k}}$ are the matrix elements quantifying the coupling to the electronic polarization. Inclusion of the anti-resonant terms in H^{el}_{bath} is straightforward, as discussed in Appendix A. In practice, $\omega^{el}_{q,\mathbf{k}}$ and $\kappa^{el}_{q,\mathbf{k}}$ can be chosen at will so as to quantitatively reproduce the properties of a specific system, in particular the frequency-dependent damping rate of the electronic excitations. A recapitulative scheme of the investigated model in depicted in Fig. 1. For a more detailed description of the specific system of semiconductor microcavities embedding intersubband transitions, the reader can refer to Refs. 4 and 9.

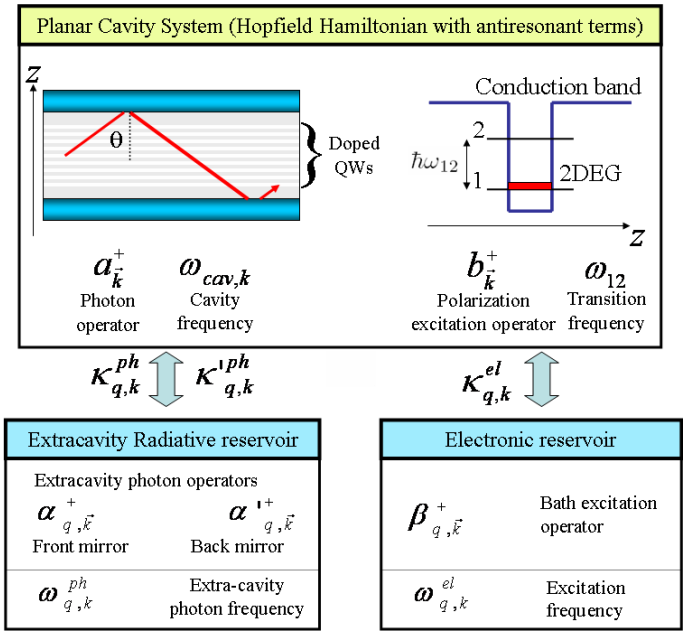

FIG. 1: A sketch of the investigated model with the corresponding operators and frequencies. The system is represented by a planar cavity mode embedding a doped multiple quantum well structure. The cavity photon field is coupled to the quantum well electronic polarization associated to a resonant intersubband transition in the doped quantum wells. The Hopfield Hamiltonian for the cavity system includes the anti-resonant light-matter interaction terms, which are significant in the ultra-strong coupling regime[9] (vacuum Rabi frequency $\Omega_{R,k}$ comparable to the transition frequency ω_{12}). The cavity mode is coupled to the extracavity electromagnetic field. The electronic polarization is coupled to a bath of electronic excitations.

II. QUANTUM DYNAMICAL EQUATIONS

A. Quantum Langevin equations

The equation of motion for the extra-cavity photon operator in Heisenberg representation reads:

$$\frac{d\alpha_{q,\mathbf{k}}}{dt} = -\frac{i}{\hbar}[\alpha_{q,\mathbf{k}}, H] = -i\omega^{ph}_{q,\mathbf{k}}\alpha_{q,\mathbf{k}} - \kappa^{ph\,*}_{q,\mathbf{k}} a_{\mathbf{k}} \ , \tag{11}$$

and its solution can be formally written as

$$\alpha_{q,\mathbf{k}}(t) = e^{-i\omega^{ph}_{q,\mathbf{k}}(t-t_0)}\alpha_{q,\mathbf{k}}(t_0) - \kappa^{ph\,*}_{q,\mathbf{k}} \int_{t_0}^{t} dt' e^{-i\omega^{ph}_{q,\mathbf{k}}(t-t')} a_{\mathbf{k}}(t') \ , \tag{12}$$

t_0 being the initial time. Inserting these formulas into the evolution equation for the cavity photon amplitude, one finds:

$$\begin{aligned}\frac{da_{\mathbf{k}}}{dt} &= -\frac{i}{\hbar}[a_{\mathbf{k}}, H_{sys}] + \int dq\ k^{ph}_{q,\mathbf{k}}\,\alpha_{q,\mathbf{k}} = \\ &= -\frac{i}{\hbar}[a_{\mathbf{k}}, H_{sys}] + \int dq\ k^{ph}_{q,\mathbf{k}}\,\alpha_{q,\mathbf{k}}(t_0)\,e^{-i\omega^{ph}_{q,\mathbf{k}}(t-t_0)} - \int dq\ |k_{q,\mathbf{k}}|^2 \int_{t_0}^{t} dt'\,e^{-i\omega^{ph}_{q,\mathbf{k}}(t-t')}\,a_{\mathbf{k}}(t') \ .\end{aligned} \tag{13}$$

Using the standard definition

$$\alpha^{in}_{q,\mathbf{k}} = \alpha_{q,\mathbf{k}}(t_0)\,e^{-i\omega^{ph}_{q,\mathbf{k}}t_0} \tag{14}$$

for the input fields at $t_0 \to -\infty$, one can cast (13) in the form of a quantum Langevin equation:

$$\frac{da_{\mathbf{k}}}{dt} = -\frac{i}{\hbar}[a_{\mathbf{k}}, H_{sys}] - \int_{-\infty}^{\infty} dt'\,\Gamma_{\mathrm{cav},\mathbf{k}}(t-t')\ a_{\mathbf{k}}(t') + F_{\mathrm{cav},\mathbf{k}}(t) \ , \tag{15}$$

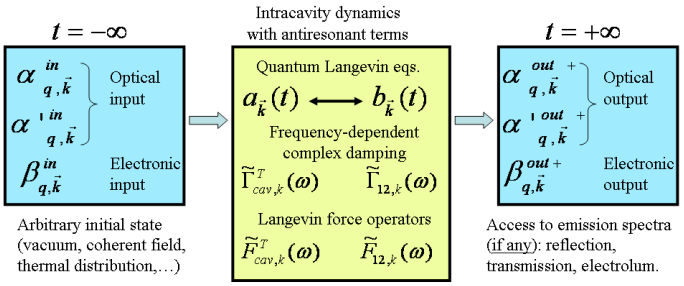

FIG. 2: A recapitulative sketch of the input-output scheme. The initial condition on the extracavity photon operators and the electronic bath operators at $t = -\infty$ represents the *input*. The intracavity dynamics for the cavity mode and electronic polarization field is described by quantum Langevin equations including the antiresonant terms of the light-matter interaction. The radiative and non-radiative baths produce a complex frequency-dependent damping as well as frequency-dependent Langevin forces. The bath operators at $t = +\infty$ represent the radiative and non-radiative *output*.

where the (causal) damping memory kernel is given by

$$\Gamma_{\mathrm{cav},\mathbf{k}}(\tau) = \Theta(\tau) \int dq \; |\kappa^{ph}_{q,\mathbf{k}}|^2 \, e^{-i\omega^{ph}_{q,\mathbf{k}}\tau} \; , \tag{16}$$

and the fluctuating Langevin force is represented by the operator

$$F_{\mathrm{cav},\mathbf{k}}(t) = \int dq \; \kappa^{ph}_{q,\mathbf{k}} e^{-i\omega^{ph}_{q,\mathbf{k}}t} \alpha^{in}_{q,\mathbf{k}} \; . \tag{17}$$

Analogously, one obtains a quantum Langevin equation for the electronic polarization field

$$\frac{\partial b_{\mathbf{k}}}{\partial t} = -\frac{i}{\hbar}[b_{\mathbf{k}}, H_{sys}] - \int_{t_0}^{\infty} dt' \Gamma_{12,\mathbf{k}}(t-t') \; b_{\mathbf{k}}(t') + F_{12,\mathbf{k}}(t) \; , \tag{18}$$

in terms of the memory kernel

$$\Gamma_{12,\mathbf{k}}(\tau) = \Theta(\tau) \int dq \; |\kappa^{el}_{q,\mathbf{k}}|^2 e^{-i\omega^{el}_{q,\mathbf{k}}\tau} \; , \tag{19}$$

and the Langevin force

$$F_{12,\mathbf{k}}(t) = \int dq \; \kappa^{el}_{q,\mathbf{k}} e^{-i\omega^{el}_{q,\mathbf{k}}t} \beta^{in}_{q,\mathbf{k}}. \tag{20}$$

The input operators $\beta^{in}_{q,\mathbf{k}}$ for the electronic bath are here defined in the same way as the photonic ones (14).

B. Input-output relations

The extra-cavity asymptotic *output* operators at $t = +\infty$ can be related to the *input* operators at $t_0 = -\infty$ and the cavity photon ones through a linear relationship. Taking $t_0 \to -\infty$ and $t \to +\infty$ in Eq. (12), we obtain the formula

$$\alpha^{out}_{q,\mathbf{k}} = \alpha^{in}_{q,\mathbf{k}} - \kappa^{ph\star}_{q,\mathbf{k}} \; \tilde{a}_{\mathbf{k}}(\omega^{ph}_{q,\mathbf{k}}), \tag{21}$$

where $\tilde{a}_{\mathbf{k}}(\omega)$ is the Fourier transform[19] of $a_{\mathbf{k}}(t)$. An analogous expression holds for the electronic bath operators:

$$\beta^{out}_{q,\mathbf{k}} = \beta^{in}_{q,\mathbf{k}} - \kappa^{el\star}_{q,\mathbf{k}} \; \tilde{b}_{\mathbf{k}}(\omega^{el}_{q,\mathbf{k}}) \tag{22}$$

C. Equations in frequency space

In the present case of a time-independent H_{sys}, the quantum Langevin equations (15) and (18) are most conveniently solved in the frequency space. By Fourier transforming them and their hermitian conjugates[19], we get the following equation

$$\bar{\mathcal{M}}_{\mathbf{k},\omega} \begin{pmatrix} \tilde{a}_{\mathbf{k}}(\omega) \\ \tilde{b}_{\mathbf{k}}(\omega) \\ \tilde{a}^{\dagger}_{-\mathbf{k}}(-\omega) \\ \tilde{b}^{\dagger}_{-\mathbf{k}}(-\omega) \end{pmatrix} + i \begin{pmatrix} \tilde{F}_{\mathrm{cav},\mathbf{k}}(\omega) \\ \tilde{F}_{12,\mathbf{k}}(\omega) \\ \tilde{F}^{\dagger}_{\mathrm{cav},-\mathbf{k}}(-\omega) \\ \tilde{F}^{\dagger}_{12,-\mathbf{k}}(-\omega) \end{pmatrix} = 0 \ , \tag{23}$$

where the 4×4 matrix

$$\bar{\mathcal{M}}_{\mathbf{k},\omega} = \begin{pmatrix} \omega_{\mathrm{cav},k} + 2D_k - \omega - i\tilde{\Gamma}_{\mathrm{cav},\mathbf{k}}(\omega) & i\Omega_{R,k} & 2D_k & -i\Omega_{R,k} \\ -i\Omega_{R,k} & \omega_{12} - \omega - i\tilde{\Gamma}_{12,\mathbf{k}}(\omega) & -i\Omega_{R,k} & 0 \\ -2D_k & -i\Omega_{R,k} & -\omega_{\mathrm{cav},k} - 2D_k - \omega - i\tilde{\Gamma}^{\star}_{\mathrm{cav},\mathbf{k}}(-\omega) & i\Omega_{R,k} \\ -i\Omega_{R,k} & 0 & -i\Omega_{R,k} & -\omega_{12} - \omega - i\tilde{\Gamma}^{\star}_{12,\mathbf{k}}(-\omega) \end{pmatrix} \tag{24}$$

is the Hopfield[9,13] matrix of our system, additioned by the terms accounting for the damping and for the frequency shift produced by the coupling to the baths. The complex self-energy shift of the cavity photon due to the coupling to the photonic bath is indeed

$$\tilde{\Gamma}_{\mathrm{cav},\mathbf{k}}(\omega) = \int dq\ \pi\, |\kappa^{ph}_{q,\mathbf{k}}|^2 \delta(\omega - \omega^{ph}_{q,\mathbf{k}}) + i\mathcal{P}\int dq\ \frac{|\kappa^{ph}_{q,\mathbf{k}}|^2}{\omega - \omega_{q,\mathbf{k}}}. \tag{25}$$

Its real part represents the frequency-dependent radiative damping of the cavity mode due to radiative losses. This, in agreement with the usual Fermi golden rule

$$\Re[\tilde{\Gamma}_{\mathrm{cav},\mathbf{k}}(\omega)] = \pi\, |k^{ph}_{\bar{q},\mathbf{k}}|^2\, \rho^{ph}_{\mathbf{k}}(\omega), \tag{26}$$

where $\rho^{ph}_{\mathbf{k}}(\omega) = \left[d\omega^{ph}_{q=\bar{q},\mathbf{k}}/dq\right]^{-1}$ is the photonic density of states at in-plane wavevector $\mathbf{k}$ and $\bar{q}$ is the resonant wavevector such that $\omega^{ph}_{\bar{q},\mathbf{k}} = \omega$. The imaginary part $\Im[\tilde{\Gamma}_{\mathrm{cav},\mathbf{k}}(\omega)]$ accounts instead for the corresponding Lamb shift[20]: for a given $\Re[\tilde{\Gamma}_{\mathrm{cav},\mathbf{k}}(\omega)]$, the Lamb shift $\Im[\tilde{\Gamma}_{\mathrm{cav},\mathbf{k}}(\omega)]$ is in fact univocally fixed by the Kramers-Kronig causality relationships

$$\Im\{\tilde{\Gamma}_{\mathrm{cav},\mathbf{k}}(\omega)\} = -\frac{1}{\pi}\mathcal{P}\ \int_{-\infty}^{\infty} d\omega' \frac{\Re\left\{\tilde{\Gamma}_{\mathrm{cav},\mathbf{k}}(\omega')\right\}}{\omega' - \omega}\ . \tag{27}$$

An analogous formula holds for the electronic excitation counterpart:

$$\tilde{\Gamma}_{12,\mathbf{k}}(\omega) = \int dq\ |\kappa^{el}_{\bar{q},\mathbf{k}}|^2 \pi\delta(\omega - \omega^{el}_{q,\mathbf{k}}) + i\mathcal{P}\int dq\ \frac{|\kappa^{el}_{q,\mathbf{k}}|^2}{\omega - \omega^{el}_{q,\mathbf{k}}}\ , \tag{28}$$

The real part of $\tilde{\Gamma}_{12,\mathbf{k}}(\omega)$ represents the frequency-dependent broadening of the electronic transition, of non-radiative origin. As all real excitations of the considered baths have by definition positive frequency $\omega^{ph,el}_{q,\mathbf{k}} > 0$, one has:

$$\Re\{\tilde{\Gamma}_{\mathrm{cav},\mathbf{k}}(\omega < 0)\} = \Re\{\tilde{\Gamma}_{12,\mathbf{k}}(\omega < 0)\} = 0\ . \tag{29}$$

In frequency space, the Langevin forces have the form

$$\tilde{F}_{\mathrm{cav},\mathbf{k}}(\omega) \ = \ \int dq\ \kappa^{ph}_{q,\mathbf{k}}\ 2\pi\delta(\omega - \omega^{ph}_{q,\mathbf{k}})\ \alpha^{in}_{q,\mathbf{k}} = 2\pi\kappa^{ph}_{\bar{q}}\,\rho^{ph}_{\mathbf{k}}(\omega)\,\alpha^{in}_{\bar{q},\mathbf{k}} \tag{30}$$

$$\tilde{F}_{12,\mathbf{k}}(\omega) \ = \ \int dq'\ \kappa^{el}_{q',\mathbf{k}}\ 2\pi\delta(\omega - \omega^{el}_{q',\mathbf{k}})\ \beta^{in}_{q',\mathbf{k}} = 2\pi\kappa^{el}_{\bar{q}'}\rho^{el}_{\mathbf{k}}(\omega)\,\beta^{in}_{\bar{q}',\mathbf{k}}, \tag{31}$$

where $\bar{q}$ and $\bar{q}'$ in the right-hand sides are such that $\omega^{ph}_{\bar{q},\mathbf{k}} = \omega^{el}_{\bar{q}',\mathbf{k}} = \omega$. In analogy with (29), one therefore has

$$\tilde{F}_{\mathrm{cav},\mathbf{k}}(\omega < 0) = \tilde{F}_{12,\mathbf{k}}(\omega < 0) = 0\ . \tag{32}$$

A recapitulative sketch of the input-output framework here developed is drawn in Fig. 2.

III. EXACT SOLUTIONS FOR THE OPERATORS

The equation (23) for the Fourier space cavity field operators is immediately solved by matrix inversion:

$$\begin{pmatrix} \tilde{a}_{\mathbf{k}}(\omega) \\ \tilde{b}_{\mathbf{k}}(\omega) \\ \tilde{a}^{\dagger}_{-\mathbf{k}}(-\omega) \\ \tilde{b}^{\dagger}_{-\mathbf{k}}(-\omega) \end{pmatrix} = \bar{\mathcal{G}}(\mathbf{k},\omega) \begin{pmatrix} \tilde{F}_{\mathrm{cav},\mathbf{k}}(\omega) \\ \tilde{F}_{12,\mathbf{k}}(\omega) \\ \tilde{F}^{\dagger}_{\mathrm{cav},-\mathbf{k}}(-\omega) \\ \tilde{F}^{\dagger}_{12,-\mathbf{k}}(-\omega) \end{pmatrix} \tag{33}$$

where

$$\bar{\mathcal{G}}(\mathbf{k},\omega) = -i\ [\bar{\mathcal{M}}_{\mathbf{k},\omega}]^{-1}\ . \tag{34}$$

For $\omega > 0$, this can be simplified as

$$\tilde{a}_{\mathbf{k}}(\omega>0) \ = \ \bar{\mathcal{G}}_{11}(\mathbf{k},\omega)\ \tilde{F}_{\mathrm{cav},\mathbf{k}}(\omega) + \bar{\mathcal{G}}_{12}(\mathbf{k},\omega)\ \tilde{F}_{12,\mathbf{k}}(\omega)\ , \tag{35}$$

$$\tilde{b}_{\mathbf{k}}(\omega>0) \ = \ \bar{\mathcal{G}}_{21}(\mathbf{k},\omega)\ \tilde{F}_{\mathrm{cav},\mathbf{k}}(\omega) + \bar{\mathcal{G}}_{22}(\mathbf{k},\omega)\ \tilde{F}_{12,\mathbf{k}}(\omega). \tag{36}$$

Using the expressions Eqs. (21-22) for the output field and the expressions (30-31) for the Langevin forces, one finally gets to the *input-output* relation:

$$\begin{pmatrix} \alpha^{out}_{q,\mathbf{k}} \\ \beta^{out}_{q',\mathbf{k}} \end{pmatrix} = \begin{pmatrix} \bar{\mathcal{U}}_{11}(\mathbf{k},\omega) & \bar{\mathcal{U}}_{12}(\mathbf{k},\omega) \\ \bar{\mathcal{U}}_{21}(\mathbf{k},\omega) & \bar{\mathcal{U}}_{22}(\mathbf{k},\omega) \end{pmatrix} \begin{pmatrix} \alpha^{in}_{q,\mathbf{k}} \\ \beta^{in}_{q',\mathbf{k}} \end{pmatrix}. \tag{37}$$

This is a linear relation linking the output operators of the photonic and electronic bath modes to the corresponding input ones; as expected by the time-invariance of the Hamiltonian under examination, the pair of photonic and electronic modes involved in (37) share by construction the same frequency $\omega^{ph}_{q,\mathbf{k}} = \omega^{el}_{q',\mathbf{k}}$. The matrix elements of $\mathcal{U}$ are

$$\bar{\mathcal{U}}_{11}(\mathbf{k},\omega) = 1 - 2\Re\{\tilde{\Gamma}_{\mathrm{cav},\mathbf{k}}(\omega)\}\bar{\mathcal{G}}_{11}(\mathbf{k},\omega)\ , \tag{38}$$

$$\bar{\mathcal{U}}_{12}(\mathbf{k},\omega) = -2\Re\{\tilde{\Gamma}_{12,\mathbf{k}}(\omega)\}\frac{\kappa^{ph\,*}_{q,\mathbf{k}}}{\kappa^{el\,*}_{q',\mathbf{k}}}\bar{\mathcal{G}}_{12}(\mathbf{k},\omega)\ , \tag{39}$$

$$\bar{\mathcal{U}}_{21}(\mathbf{k},\omega) = -2\Re\{\tilde{\Gamma}_{\mathrm{cav},\mathbf{k}}(\omega)\}\frac{\kappa^{el\,*}_{q',\mathbf{k}}}{\kappa^{ph\,*}_{q,\mathbf{k}}}\bar{\mathcal{G}}_{21}(\mathbf{k},\omega)\ , \tag{40}$$

$$\bar{\mathcal{U}}_{22}(\mathbf{k},\omega) = 1 - 2\Re\{\tilde{\Gamma}_{12,\mathbf{k}}(\omega)\}\bar{\mathcal{G}}_{22}(\mathbf{k},\omega)\ . \tag{41}$$

The unitarity of the matrix $\bar{\mathcal{U}}(\mathbf{k},\omega)$ (that has been numerically checked) guarantees that the usual Bose commutation rules hold for the output operators $\alpha^{out}_{q,\mathbf{k}}$ and $\beta^{out}_{q,\mathbf{k}}$, namely $[\alpha^{out}_{q,\mathbf{k}}, \alpha^{out\,\dagger}_{q',\mathbf{k}'}] = \delta(q-q')\,\delta_{\mathbf{k},\mathbf{k}'}$ and $[\beta^{out}_{q,\mathbf{k}}, \beta^{out\,\dagger}_{q',\mathbf{k}'}] = \delta(q-q')\,\delta_{\mathbf{k},\mathbf{k}'}$. ¿From a more physical point of view, the unitarity of $\bar{\mathcal{U}}(\mathbf{k},\omega)$ means that the total energy is conserved during a scattering process when energy is sent onto the cavity as radiation or as electronic energy, and both the emerging light and the electronic absorption are taken into account:

$$\left\langle \alpha^{out\,\dagger}_{q,\mathbf{k}}\ \alpha^{out}_{q,\mathbf{k}} + \beta^{out\,\dagger}_{q',\mathbf{k}}\ \beta^{out}_{q',\mathbf{k}} \right\rangle = \left\langle \alpha^{in\,\dagger}_{q,\mathbf{k}}\ \alpha^{in}_{q,\mathbf{k}} + \beta^{in\,\dagger}_{q',\mathbf{k}}\ \beta^{in}_{q',\mathbf{k}} \right\rangle \tag{42}$$

It is interesting and an important check of consistency to verify that the usual commutation rules $[a_{\mathbf{k}}(t), a^{\dagger}_{\mathbf{k}'}(t)] = \delta_{\mathbf{k},\mathbf{k}'}$ hold for the cavity (as well as for the electronic polarization) operators. This has been verified on our specific model in the following way. By definition, one has:

$$[a_{\mathbf{k}}(t), a^{\dagger}_{\mathbf{k}'}(t)] = \int \frac{d\omega}{2\pi} \int \frac{d\omega'}{2\pi}\, e^{-i\omega t}\, e^{i\omega' t}\, [\tilde{a}_{\mathbf{k}}(\omega), \tilde{a}^{\dagger}_{\mathbf{k}'}(\omega')]. \tag{43}$$

Inserting here (33), and noticing that

$$[\tilde{F}_{\mathrm{cav},\mathbf{k}}(\omega), \tilde{F}^{\dagger}_{\mathrm{cav},\mathbf{k}'}(\omega')] = 2\pi\,\delta(\omega-\omega')\,2\,\Re[\tilde{\Gamma}_{\mathrm{cav},\mathbf{k}}(\omega)]\,\delta_{\mathbf{k},\mathbf{k}'}, \tag{44}$$

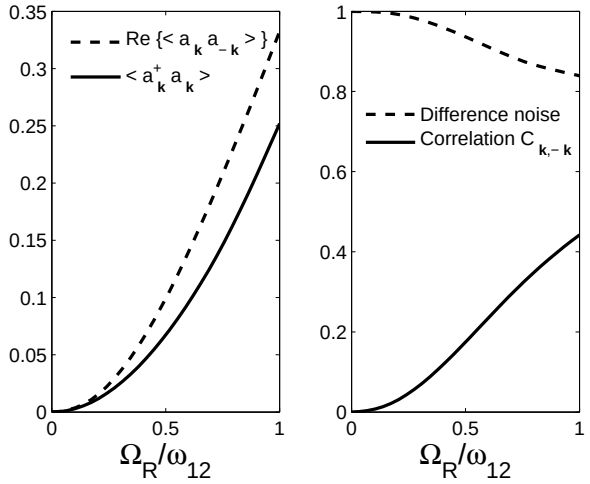

FIG. 3: Quantum properties of the intra-cavity ground state for input fields in the vacuum state. In this case, the output is also in the vacuum state, which implies that the cavity photons present in the cavity are purely virtual ones and can not escape the cavity. Left panel: cavity photon number $\langle a^\dagger_{\mathbf{k}} a_{\mathbf{k}}\rangle$ (solid line) and the real part of the anomalous expectation value $\langle a_{\mathbf{k}} a_{-\mathbf{k}}\rangle$ (dashed line) as a function of the normalized vacuum Rabi frequency Ω_R/ω_{12}. Right panel: corresponding cavity photon correlation $C_{\mathbf{k},-\mathbf{k}}$ (solid line) and the normalized difference noise $F_{\rm diff}$ (dashed line). $\omega_{{\rm cav},k} = \omega_{12}$, and the damping rates are taken as frequency-independent ones. The calculations have been performed with $\Re\{\Gamma_{{\rm cav},\mathbf{k}}(\omega > 0)\} = \bar\Gamma_{{\rm cav},k} = \Re\{\Gamma'_{{\rm cav},\mathbf{k}}(\omega > 0)\} = \bar\Gamma'_{{\rm cav},k} = 0.04\omega_{12}$ and $\Re\{\Gamma_{12,k}(\omega > 0)\} = \bar\Gamma_{12,k} = 0.08\omega_{12}$.

one can finally write:

$$[a(t), a^\dagger(t)] = 2\int \frac{d\omega}{2\pi}\Big[|\bar{\mathcal{G}}_{11}(\mathbf{k},\omega)|^2\,\Re[\tilde\Gamma_{{\rm cav},\mathbf{k}}(\mathbf{k},\omega)] + |\bar{\mathcal{G}}_{12}(\mathbf{k},\omega)|^2\,\Re[\tilde\Gamma_{12,\mathbf{k}}(\omega)] + \\ - |\bar{\mathcal{G}}_{13}(\mathbf{k},\omega)|^2\,\Re[\tilde\Gamma_{{\rm cav},\mathbf{k}}(-\omega)] - |\bar{\mathcal{G}}_{14}(\mathbf{k},\omega)|^2\,\Re[\tilde\Gamma_{12,\mathbf{k}}(-\omega)]\Big], \quad (45)$$

which has been numerically checked to give 1 as expected. This fact critically depends on the consistent inclusion of the real and imaginary parts of $\tilde\Gamma_{{\rm cav},\mathbf{k}}(\omega)$ and $\tilde\Gamma_{12,\mathbf{k}}(\omega)$ satisfying the causality relation (27).

Note finally that the presence of the anti-resonant terms in H_{sys} implies that the cavity operators $\tilde a_{\mathbf{k}}(\omega)$ and $\tilde b_{\mathbf{k}}(\omega)$ have non-vanishing values also for negative frequencies:

$$\tilde a_{\mathbf{k}}(\omega < 0) \;=\; \bar{\mathcal{G}}_{13}(\mathbf{k},\omega)\;\tilde F^\dagger_{{\rm cav},-\mathbf{k}}(-\omega) + \bar{\mathcal{G}}_{14}(\mathbf{k},\omega)\;\tilde F^\dagger_{12,-\mathbf{k}}(-\omega) \quad (46)$$

$$\tilde b_{\mathbf{k}}(\omega < 0) \;=\; \bar{\mathcal{G}}_{23}(\mathbf{k},\omega)\;\tilde F^\dagger_{{\rm cav},-\mathbf{k}}(-\omega) + \bar{\mathcal{G}}_{24}(\mathbf{k},\omega)\;\tilde F^\dagger_{12,-\mathbf{k}}(-\omega)\;. \quad (47)$$

IV. THE CASE OF A VACUUM INPUT: PROPERTIES OF THE INTRACAVITY QUANTUM GROUND STATE

Once we have obtained explicit expressions for the output operators in terms of the input ones, we can apply this formalism to study the quantum dissipative response of the cavity system for different initial states.

We shall start from the simplest case of a bath initially in its vacuum state $|0\rangle$ such that:

$$\alpha^{in}_{q,\mathbf{k}}|0\rangle = \beta^{in}_{q,\mathbf{k}}|0\rangle = 0 \quad (48)$$

for every $\mathbf{k}$ and q. As expected on physical grounds, no excitations are created, and the bath remains in its vacuum state. It is in fact a straightforward consequence of (37) that

$$\alpha^{out}_{q,\mathbf{k}}|0\rangle = \beta^{out}_{q,\mathbf{k}}|0\rangle = 0. \quad (49)$$

On the other hand, the cavity system itself is not in the usual vacuum state, and a finite number of photons is present in this anomalous ground state. This can be calculated by means of (33), which relates the in-cavity field $a_{\mathbf{k}}$ to the

input bath operators $F_{\mathrm{cav},12}$ and $F^\dagger_{\mathrm{cav},12}$:

$$\left\langle a^\dagger_{\mathbf{k}}(t)a_{\mathbf{k}}(t)\right\rangle = \frac{1}{(2\pi)^2}\int_{-\infty}^{\infty}d\omega\int_{-\infty}^{\infty}d\omega'\ \left\langle \tilde{a}^\dagger_{\mathbf{k}}(\omega)\tilde{a}_{\mathbf{k}}(\omega')\right\rangle\ e^{-i(\omega-\omega')t} = \\ = \frac{1}{\pi}\int_0^\infty d\omega|\bar{\mathcal{G}}_{13}(\mathbf{k},-\omega)|^2\Re\{\tilde{\Gamma}_{\mathrm{cav},\mathbf{k}}(\omega)\} + |\bar{\mathcal{G}}_{14}(\mathbf{k},-\omega)|^2\Re\{\tilde{\Gamma}_{12,\mathbf{k}}(\omega)\}. \quad (50)$$

As the input bath is here taken in the vacuum state $F_{\mathrm{cav},12}\left|0\right\rangle = 0$, only the terms involving $F^\dagger_{\mathrm{cav},12}$ contribute to the result (50). The presence of the anti-resonant light-matter coupling H_{anti} is here crucial, as it is responsible for the non-vanishing value of the matrix elements $\mathcal{G}_{13}$ and $\bar{\mathcal{G}}_{14}$ connecting creation and destruction operators.

Remarkably, the ground state shows finite *anomalous* correlations between modes with opposite wavevectors:

$$\langle a_{\mathbf{k}}(t)a_{-\mathbf{k}}(t)\rangle = \frac{1}{(2\pi)^2}\int_{-\infty}^{\infty}d\omega\int_{-\infty}^{\infty}d\omega'\ \left\langle \tilde{a}^\dagger_{\mathbf{k}}(\omega)\tilde{a}_{\mathbf{k}}(\omega')\right\rangle\ e^{i(\omega+\omega')t} = \\ = \frac{1}{\pi}\int_0^\infty d\omega\,\bar{\mathcal{G}}_{11}(\mathbf{k},\omega)\bar{\mathcal{G}}_{13}(-\mathbf{k},-\omega)\Re\{\tilde{\Gamma}_{\mathrm{cav},\mathbf{k}}(\omega)\} + \bar{\mathcal{G}}_{22}(\mathbf{k},\omega)\bar{\mathcal{G}}_{14}(-\mathbf{k},-\omega)\Re\{\tilde{\Gamma}_{12,\mathbf{k}}(\omega)\}\ , \quad (51)$$

which suggest the ground state to be a sort of squeezed vacuum.

The predictions (50) and (51) for respectively the number of photons (solid line) and the anomalous correlations (dashed line) have been plotted in the left panel of Fig. 3 as a function of the normalized vacuum Rabi frequency Ω_R/ω_{12} for the resonant case $\omega_{\mathrm{cav},k} = \omega_{12}$. For simplicity, in Fig.3 as well as in all the following figures, a frequency-independent damping of the cavity and electronic excitation modes has been used, i.e., $\Re\{\Gamma_{\mathrm{cav},\mathbf{k}}(\omega>0)\} = \bar{\Gamma}_{\mathrm{cav},k}$ and $\Re\{\Gamma_{12,\mathbf{k}}(\omega>0)\} = \bar{\Gamma}_{12,k}$. Note, however, that our theory is able to describe the system under consideration for colored baths with an arbitrary frequency dependence of $\Gamma_{\mathrm{cav},\mathbf{k}}(\omega)$ and $\Gamma_{12,\mathbf{k}}(\omega)$.

It is interesting to check that in the limit $\tilde{\Gamma}_{\mathrm{cav},\mathbf{k}}, \tilde{\Gamma}_{12,\mathbf{k}} \to 0$ the values of (50) and (51) are in quantitative agreement with the result of a direct diagonalization of the isolated cavity Hamiltonian H_{sys} as done in Ref.9. Up to moderate values of the broadening values, the difference from the isolated cavity preduction remains small, in particular the total number of virtual photons is only slightly changed.

Insight on the structure of the ground state can be obtained by looking at other observables which are most sensitive to two-mode squeezing effects. In the right panel of Fig. 3 we have shown the results for the photonic correlation $C_{\mathbf{k},-\mathbf{k}}$ (solid line) between the noise amplitudes of the $\mathbf{k}$ and $-\mathbf{k}$-modes. As usual, the amplitude quadrature operator of the $\mathbf{k}$-mode is defined as $\hat{X}_{\mathbf{k}} = a_{\mathbf{k}} + a^\dagger_{\mathbf{k}}$. In the ground state, this correlation is

$$C_{\mathbf{k},-\mathbf{k}} = \frac{\langle(\hat{X}_{\mathbf{k}} - \langle\hat{X}_{\mathbf{k}}\rangle)(\hat{X}_{-\mathbf{k}} - \langle\hat{X}_{-\mathbf{k}}\rangle)\rangle}{\sqrt{\langle(\hat{X}_{\mathbf{k}} - \langle\hat{X}_{\mathbf{k}}\rangle)^2\rangle\langle(\hat{X}_{-\mathbf{k}} - \langle\hat{X}_{-\mathbf{k}}\rangle)^2\rangle}} = \frac{2\Re\{\langle a_{\mathbf{k}}a_{-\mathbf{k}}\rangle\}}{1+2\langle a^\dagger_{\mathbf{k}}a_{\mathbf{k}}\rangle}\ , \quad (52)$$

where we have used the fact that in the ground state $\langle\hat{X}_{\mathbf{k}}\rangle = \langle\hat{X}_{-\mathbf{k}}\rangle = 0$. As shown in right panel of Fig. 3, the correlation tends to 0 when $\Omega_R/\omega_{12} \to 0$, i.e., the normal vacuum is reobtained in the weak-coupling limit.

In the right panel of Fig. 3, the normalized variance of the difference between the amplitude quadratures of two correlated modes is shown, namely

$$F_{\mathrm{diff}} = \frac{1}{2}\ \langle(\hat{X}_{\mathbf{k}} - \hat{X}_{-\mathbf{k}})^2\rangle\ = 1 + 2\langle a^\dagger_{\mathbf{k}}a_{\mathbf{k}}\rangle - 2\Re\{\langle a_{\mathbf{k}}a_{-\mathbf{k}}\rangle\}\ . \quad (53)$$

Fluctuations below the shot noise level correspond to $F_{\mathrm{diff}} < 1$. As shown in the figure, F_{diff} tends to 1 for vanishing Ω_R/ω_{12}. When entering the ultra-strong coupling regime, F_{diff} decreases, becoming smaller than 1 and the two-mode squeezing of the quantum ground state becomes more and more significant.

It is important to stress that the discussion in the present section involves the state of the intra-cavity field, and that the virtual photonic and electronic excitations present in the cavity ground state are trapped inside the cavity. For an input field in the vacuum state, the output is in fact always in the vacuum state as well and no radiation will be emitted, in agreement with energy consevation requirements. On the other hand, if the properties of the cavity system were modulated in time in a non-adiabatic way, a creation of real excitations is possible inside the cavity, which in turn leads to a finite emission of *quantum vacuum radiation*[9] analogous to what is predicted to happen in the so-called dynamical Casimir effect[24,25]. A complete study of these issues, and in particular of the emission intensity, is presently the subject of detailed investigations[26].

V. EXTRACAVITY TWO-MODE SQUEEZING FROM A NON-SQUEEZED OPTICAL INPUT ?

An interesting question which has been raised in the literature of interband excitonic transitions[27,28,29] is whether any quantum optical squeezing[12] can be observed as a consequence of the finite anomalous correlation shown by the polariton vacuum[13]. In our specific case, the question we ask is whether the finite anomalous correlations (51) shown by the intracavity photon field can be observed as a squeezing of the output field emitted by the cavity. This, obviously, in the absence of any squeezing in the input field.

The most general non-squeezed optical input state is identified by the condition:

$$\left\langle \alpha^{in}_{q,\mathbf{k}}\, \alpha^{in}_{q',\mathbf{k}'} \right\rangle - \left\langle \alpha^{in}_{q,\mathbf{k}} \right\rangle \left\langle \alpha^{in}_{q',\mathbf{k}'} \right\rangle = 0, \tag{54}$$

which is well satisfied by a thermal incident state, as well as by a coherent incident field[12]. The electronic input is assumed to be in a thermal state and to have no correlations with the optical input.

As Eq. (37) relates the annihilation operators of the output to the annihilation operators of the input without involving the creation ones, one has:

$$\left\langle \alpha^{out}_{q,\mathbf{k}} \right\rangle \;=\; \bar{\mathcal{U}}_{11}(\mathbf{k}, \omega = \omega^{ph}_{q,\mathbf{k}}) \left\langle \alpha^{in}_{q,\mathbf{k}} \right\rangle \tag{55}$$

$$\left\langle \alpha^{out}_{q,\mathbf{k}}\, \alpha^{out}_{q',\mathbf{k}'} \right\rangle \;=\; \bar{\mathcal{U}}_{11}(\mathbf{k}, \omega = \omega^{ph}_{q,\mathbf{k}}) \bar{\mathcal{U}}_{11}(\mathbf{k}, \omega = \omega^{ph}_{q',\mathbf{k}'}) \left\langle \alpha^{in}_{q,\mathbf{k}}\, \alpha^{in}_{q',\mathbf{k}'} \right\rangle \;, \tag{56}$$

from which it is immediate to prove that no squeezing is present in the the output field either:

$$\left\langle \alpha^{out}_{q,\mathbf{k}}\, \alpha^{out}_{q',\mathbf{k}'} \right\rangle - \left\langle \alpha^{out}_{q,\mathbf{k}} \right\rangle \left\langle \alpha^{out}_{q',\mathbf{k}'} \right\rangle = 0. \tag{57}$$

This answers our initial question: no squeezing can be ever observed in the output unless the input field is itself squeezed, or the properties of the cavity are modulated in time.

VI. OPTICAL SPECTRA

So far, the discussion has been limited to the case of a single photonic bath coupled to the cavity. This model is sufficient to describe a single-sided cavity in which the cavity mode is coupled to the radiative modes through only one of its mirrors, while the other one is supposed to be perfectly reflecting. In order to obtain quantitative predictions for quantities of actual experimental interest like reflection, transmission and absorption spectra, one has to generalize the model adding a second photonic bath so as to include the radiation emitted by the cavity through its back mirror, as sketched in Fig.1.

A. Double-sided cavity: general theory

The total Hamiltonian must now include a second photonic bath associated to the radiation in the half-space behind the cavity, which is coupled to the cavity mode through the back mirror. This can be done by simply including another term analogous to (10):

$$H^{ph'}_{bath} = \int dq \sum_{\mathbf{k}} \hbar \omega^{ph}_{q,\mathbf{k}} \left(\alpha'^{\dagger}_{q,\mathbf{k}} \alpha'_{q,\mathbf{k}} + \frac{1}{2} \right) + i\hbar \int dq \sum_{\mathbf{k}} \left[\kappa^{ph'}_{q,\mathbf{k}}\, \alpha'_{q,\mathbf{k}}\, a^{\dagger}_{\mathbf{k}} - \kappa^{ph'\,*}_{q,\mathbf{k}}\, \alpha'^{\dagger}_{q,\mathbf{k}}\, a_{\mathbf{k}} \right]. \tag{58}$$

The new Hopfield matrix $\bar{\mathcal{M}}^{double}_{\mathbf{k},\omega}$ is obtained by $\bar{\mathcal{M}}_{\mathbf{k},\omega}$ in (24) by simply replacing:

$$\tilde{\Gamma}_{\mathrm{cav},\mathbf{k}}(\omega) \rightarrow \tilde{\Gamma}^{T}_{\mathrm{cav},\mathbf{k}}(\omega) = \tilde{\Gamma}_{\mathrm{cav},\mathbf{k}}(\omega) + \tilde{\Gamma}'_{\mathrm{cav},\mathbf{k}}(\omega) \;, \tag{59}$$

where $\tilde{\Gamma}'_{\mathrm{cav},\mathbf{k}}(\omega)$ is the complex linewidth of the cavity mode due to the finite transmittivity of the second mirror, defined in a way analogous to the definition (25) of $\tilde{\Gamma}_{\mathrm{cav},\mathbf{k}}(\omega)$. Correspondingly, a new Langevin force $F'_{\mathrm{cav},\mathbf{k}}(t)$ analogous to (17) has to be included, which means to replace in (33)

$$\tilde{F}_{\mathrm{cav},\mathbf{k}}(\omega) \rightarrow \tilde{F}^{T}_{\mathrm{cav},\mathbf{k}}(\omega) = \tilde{F}_{\mathrm{cav},\mathbf{k}}(\omega) + \tilde{F}'_{\mathrm{cav},\mathbf{k}}(\omega) \;. \tag{60}$$

Following the same steps as in the case of the one-sided cavity, the solutions for the output operators are

$$\begin{pmatrix} \alpha^{out}_{q,\mathbf{k}} \\ \beta^{out}_{q',\mathbf{k}} \\ \alpha'^{out}_{q,\mathbf{k}} \end{pmatrix} = \mathcal{U}^{double}(\mathbf{k}, \omega) \begin{pmatrix} \alpha^{in}_{q,\mathbf{k}} \\ \beta^{in}_{q',\mathbf{k}} \\ \alpha'^{in}_{q,\mathbf{k}} \end{pmatrix} \;, \tag{61}$$

where $\mathcal{U}^{double}(\mathbf{k},\omega)$ is a 3×3 unitary matrix. Similarly to the single-sided case of (38-41), its matrix elements can be written as:

$$\bar{\mathcal{U}}^{double}_{jl}(\mathbf{k},\omega) = \delta_{jl} - 2\Re\{\tilde{\Gamma}_{l,\mathbf{k}}(\omega)\}\left(\frac{\kappa^{j}_{q,\mathbf{k}}}{\kappa^{l}_{q',\mathbf{k}}}\right)^{*} \bar{\mathcal{G}}^{double}_{jl}(\mathbf{k},\omega)\ . \tag{62}$$

Here, a shorthand notation has been used: for $j=\{1,2,3\}$, the quantities $\tilde{\Gamma}_{j,\mathbf{k}}(\omega)$ respectively mean $\tilde{\Gamma}_{\mathrm{cav},\mathbf{k}}(\omega)$, $\tilde{\Gamma}_{12,\mathbf{k}}(\omega)$, and $\tilde{\Gamma}'_{\mathrm{cav},\mathbf{k}}(\omega)$. Analogously, $\kappa^{j}_{q,\mathbf{k}}$ respectively mean $\kappa^{ph}_{q,\mathbf{k}}$, $\kappa^{el}_{q,\mathbf{k}}$, and $\kappa'^{ph}_{q,\mathbf{k}}$ and all the three are evaluated at wavevector values such that $\omega^{ph}_{q,\mathbf{k}} = \omega^{el}_{q',\mathbf{k}} = \omega$. $\bar{\mathcal{G}}^{double}(\mathbf{k},\omega)$ is defined as $\bar{\mathcal{G}}^{double}(\mathbf{k},\omega) = -i\ [\bar{\mathcal{M}}^{double}_{\mathbf{k},\omega}]^{-1}$.

In the single-sided cavity limit, one has $\bar{\mathcal{U}}^{double}_{jk}(\mathbf{k},\omega) = \bar{\mathcal{U}}_{jk}(\mathbf{k},\omega)$ and $\bar{\mathcal{U}}^{double}_{j3}(\mathbf{k},\omega) = \bar{\mathcal{U}}^{double}_{3j}(\mathbf{k},\omega) = 0$ for $j,k=\{1,2\}$, and $\bar{\mathcal{U}}^{double}_{33}(\mathbf{k},\omega) = 1$.

B. Linear optical spectra

The results of the previous subsection can be used to obtain quantitative predictions for the optical properties of the cavity, namely its reflection, absorption and transmission spectra as a function of the frequency ω of the incident light. Here, we assume that no input other than optical is present, i.e., $\langle \beta^{in,\dagger}_{q,\mathbf{k}}\ \beta^{in}_{q,\mathbf{k}}\rangle = 0$, and that the coherent radiation incides onto the cavity from the half-space in front of it, i.e. $\langle \alpha^{in,\dagger}_{q,\mathbf{k}}\ \alpha^{in}_{q,\mathbf{k}}\rangle > 0$, while $\langle \alpha'^{in,\dagger}_{q,\mathbf{k}}\ \alpha'^{in}_{q,\mathbf{k}}\rangle = 0$.

In the considered geometry, reflection is described by the output operator $\alpha^{out}_{q,\mathbf{k}}$, so that the reflectivity is equal to

$$\mathcal{R}_{\mathbf{k}}(\omega) = \frac{\langle \alpha^{out\dagger}_{q,\mathbf{k}}\ \alpha^{out}_{q,\mathbf{k}}\rangle}{\langle \alpha^{in\dagger}_{q,\mathbf{k}}\ \alpha^{in}_{q,\mathbf{k}}\rangle} = |\bar{\mathcal{U}}^{double}_{11}(\mathbf{k},\omega)|^2\ . \tag{63}$$

The transmission through the second mirror is described by the output operator $\alpha'^{out}_{q,\mathbf{k}}$. Therefore, the transmittivity reads

$$\mathcal{T}_{\mathbf{k}}(\omega) = \frac{\langle \alpha'^{out\dagger}_{q,\mathbf{k}}\ \alpha'^{out}_{q,\mathbf{k}}\rangle}{\langle \alpha^{in\dagger}_{q,\mathbf{k}}\ \alpha^{in}_{q,\mathbf{k}}\rangle} = |\bar{\mathcal{U}}^{double}_{31}(\mathbf{k},\omega)|^2\ . \tag{64}$$

Note that $\mathcal{T}_{\mathbf{k}}(\omega) = 0$ in the single-sided case. The presence of the electronic bath implies that the incident light can be absorbed into electronic energy. The corresponding absorption coefficient of the microcavity system is:

$$\mathcal{A}_{\mathbf{k}}(\omega) = |\bar{\mathcal{U}}^{double}_{21}(\mathbf{k},\omega)|^2\ . \tag{65}$$

As expected, the total energy is conserved, i.e. $\mathcal{R}_{\mathbf{k}}(\omega) + \mathcal{A}_{\mathbf{k}}(\omega) + \mathcal{T}_{\mathbf{k}}(\omega) = 1$, as one can verify from the unitarity of $\bar{\mathcal{U}}^{double}(\mathbf{k},\omega)$.

In Fig. 4, we show an example of reflectivity, transmission, and absorption spectra for different values of the normalized detuning $\delta = (\omega_{\mathrm{cav},k} - \omega_{12})/\omega_{12}$, which is varied from -0.5 to 0.5 by steps equal to 0.1. The linear optical spectra have resonances corresponding to the cavity polariton eigenmodes. For the large vacuum Rabi frequency here considered ($\Omega_R = 0.4\omega_{12}$), it is apparent that the optical spectra show an anticrossing of the polariton eigenmodes, which is is strongly asymmetric, as it was anticipated in the case of a closed cavity system[9] without dissipation. This can be also seen in Fig. 5, showing the reflection, transmission, and absorption spectra for zero detuning ($\omega_{\mathrm{cav},k} = \omega_{12}$) and increasing values of Ω_R/ω_{12} (from 0 to 0.5 with steps of 0.05). Remarkably, note that for an incident frequency close to resonance with the polariton eigenmodes, a significative fraction of the incident energy goes is dissipated in the electronic bath as absorption.

C. Electroluminescence

Another physical quantity which can be successfully studied by the present theory is the intensity of the light emitted by the cavity when this is incoherently excited from the electronic bath in a so-called *electroluminescence* experiment. Electrically excited intersubband transitions are in fact playing an important role as light sources in the mid and in the far infrared region, but they still suffer from a poor quantum efficiency of radiative emission as compared to non-radiative losses. A way of enhancing the emission efficiency would therefore be of great interest.

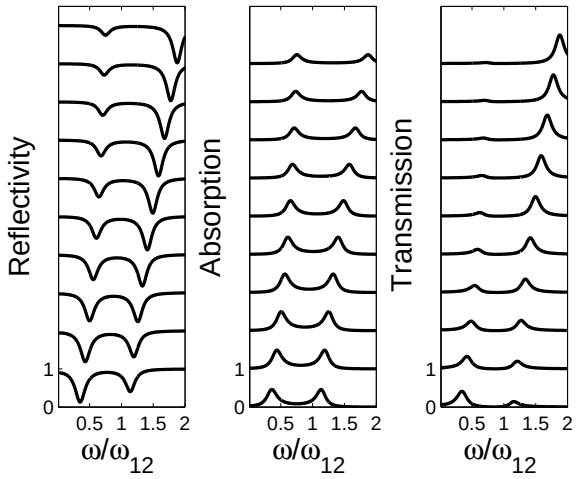

FIG. 4: Reflectivity $\mathcal{R}_{\mathbf{k}}(\omega)$ (left), absorption $\mathcal{A}_{\mathbf{k}}(\omega)$ (center) and transmission $\mathcal{T}_{\mathbf{k}}(\omega)$ (right) spectra as a function of the normalized photon frequency ω/ω_{12} for different values of the normalized detuning $\delta = (\omega_{\mathrm{cav},k} - \omega_{12})/\omega_{12}$ (from $\delta = -0.5$ to $\delta = +0.5$ by steps of 0.1). The different curves are offset for clarity. The bottom curve corresponds to $\delta = -0.5$, while the top one has been obtained for $\delta = 0.5$. Parameters: $\Omega_{R,k}/\omega_{12} = 0.4$. Broadening parameters as in Fig. 3

.

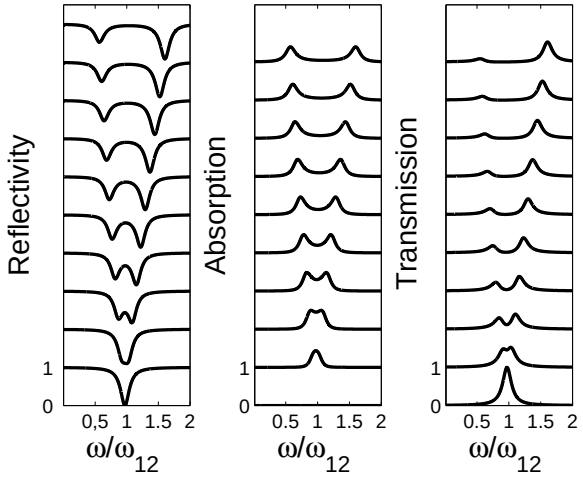

FIG. 5: Reflectivity $\mathcal{R}_{\mathbf{k}}(\omega)$ (left), absorption $\mathcal{A}_{\mathbf{k}}(\omega)$ (center) and transmittivity $\mathcal{T}_{\mathbf{k}}(\omega)$ (right) spectra as a function of the normalized photon frequency ω/ω_{12} for different values of the normalized vacuum Rabi frequency Ω_R/ω_{12} for the resonant case $\omega_{\mathrm{cav},k} = \omega_{12}$. The different curves are offset for clarity. The bottom curve corresponds to $\Omega_R = 0$, while the top curve corresponds to $\Omega_R = 0.5\omega_{12}$ (Ω_R/ω_{12} is increased by steps of 0.05). Same broadening parameters as in Fig.4.

Consider a purely electronic, incoherent input, distributed among the different q modes:

$$\langle \beta^{in,\dagger}_{q,\mathbf{k}} \ \beta^{in}_{q,\mathbf{k}} \rangle \ = \ I^{el}_{exc,q} > 0 \ , \tag{66}$$

$$\langle \alpha'^{in,\dagger}_{q,\mathbf{k}} \ \alpha'^{in}_{q,\mathbf{k}} \rangle \ = \ \langle \alpha'^{in,\dagger}_{q,\mathbf{k}} \ \alpha'^{in}_{q,\mathbf{k}} \rangle = 0. \tag{67}$$

The intensity of the spontaneously emitted light through the front mirror (defined as the mean number of photons in the q mode) is proportional to the quantity

$$\mathcal{L}_{\mathbf{k}} = \ \int dq \ \langle \alpha^{out,\dagger}_{q,\mathbf{k}} \ \alpha^{out}_{q,\mathbf{k}} \rangle = \int d\omega \ \rho^{ph}_{\mathbf{k}}(\omega) \ |\bar{\mathcal{U}}^{double}_{12}(\mathbf{k},\omega)|^2 I^{el}_{exc}(\omega). \tag{68}$$

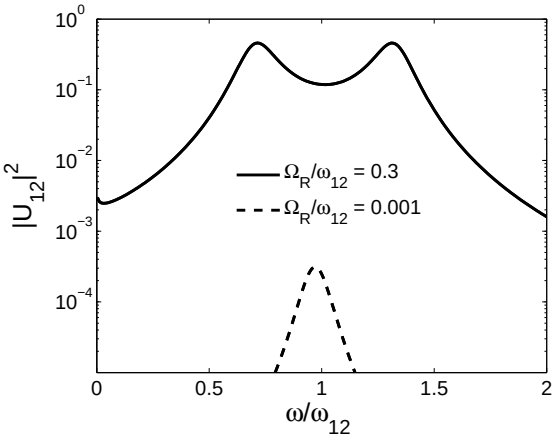

FIG. 6: A logarithmic scale plot of the dimensionless quantity $|\bar{\mathcal{U}}_{12}^{double}(\mathbf{k},\omega)|^2$ (proportional to the electroluminescence spectrum) as a function of the normalized frequency ω/ω_{12} in a weak-coupling regime $\Omega_R/\omega_{12} = 0.001$ (dashed-line) and in a strong-coupling one $\Omega_R/\omega_{12} = 0.3$ (solid line). Other parameters as in Fig. 5. The small increase at very low ω is a consequence of the specific choice of constant values for $\Re\{\bar{\Gamma}_{\mathrm{cav},\mathbf{k}}(\omega > 0)\}$ and $\Re\{\bar{\Gamma}_{12,\mathbf{k}}(\omega > 0)\}$, producing a Kramers-Kronig singularity of the imaginary part (Lamb shift) at $\omega = 0$.

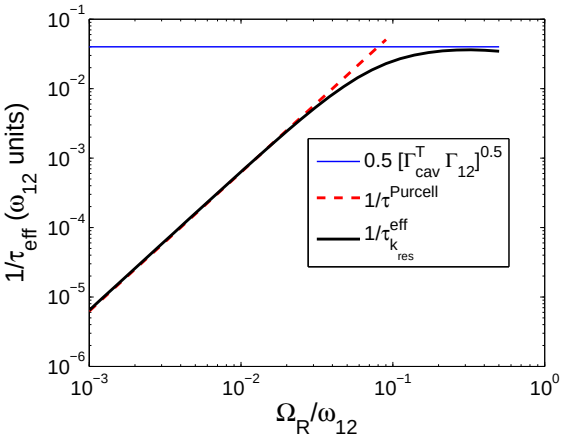

FIG. 7: Solid line: the effective spontaneous emission rate γ_k^{eff} (in units of ω_{12}) as a function of the normalized vacuum Rabi frequency $\Omega_{R,k}/\omega_{12}$ for $\omega_{\mathrm{cav},k} = \omega_{12}$. Dashed-line: the Purcell rate $2\frac{\bar{\Gamma}_{\mathrm{cav}}}{\bar{\Gamma}^T_{\mathrm{cav}}}\frac{\Omega^2_{R,k}}{\bar{\Gamma}^T_{\mathrm{cav}}+\bar{\Gamma}_{12}}$. Horizontal line: the strong coupling limit $\frac{1}{2}\sqrt{\Gamma^T_{\mathrm{cav}}\Gamma_{12}}$. Parameters: $\bar{\Gamma}_{\mathrm{cav},\mathbf{k}} = \bar{\Gamma}'_{\mathrm{cav},\mathbf{k}} = 0.04\omega_{12}$ and $\bar{\Gamma}_{12,\mathbf{k}} = 0.08\omega_{12}$.

The dimensionless quantity $|\bar{\mathcal{U}}_{12}^{double}(\mathbf{k},\omega)|^2$ is represented in Fig. 6 for a weak-coupling situation (dashed-line) and for a strong coupling case (solid line), where it exhibits two polaritonic resonances. Suppose that in the spectral region where $|\bar{\mathcal{U}}_{12}^{double}(\mathbf{k},\omega)|^2$ is significant we can roughly neglect the frequency-dependence of the electronic excitation ($I^{el}_{exc}(\omega) \approx I^{el}_{exc}$) and of the extracavity photon density of state ($\rho^{ph}_{\mathbf{k}}(\omega) \approx \rho^{ph}_{\mathbf{k}}$). With these approximations, the luminescence intensity is given by the simplified expression

$$\mathcal{L}_{\mathbf{k}} \approx \rho^{ph}_{\mathbf{k}} I^{el}_{exc} \gamma^{\mathrm{eff}}_{\mathbf{k}} \ , \tag{69}$$

where the effective rate of the luminescence is

$$\gamma^{\mathrm{eff}}_{\mathbf{k}} = \int d\omega \ |\bar{\mathcal{U}}_{12}^{double}(\mathbf{k},\omega)|^2. \tag{70}$$

If we further neglect the frequency-dependence of the broadening, (i.e. $\Re\{\Gamma_{\mathrm{cav},\mathbf{k}}(\omega > 0)\} \approx \bar{\Gamma}^T_{\mathrm{cav},\mathbf{k}}$, $\Re\{\Gamma_{12,\mathbf{k}}(\omega > 0)\} \approx \bar{\Gamma}_{12,\mathbf{k}}$) and consider the resonant case $\omega_{\mathrm{cav},k} = \omega_{12}$, the results can be expressed by simple analytical expressions.

In the weak-coupling regime $\Omega_{R,k}^2 \ll \bar{\Gamma}_{\mathrm{cav},\mathbf{k}}^T \bar{\Gamma}_{12,\mathbf{k}}$, it can be accurately approximated by a Purcell-like[30,31] law:

$$\gamma_{\mathbf{k}}^{\mathrm{eff}} \simeq 2\,\frac{\bar{\Gamma}_{\mathrm{cav},\mathbf{k}}}{\bar{\Gamma}_{\mathrm{cav},\mathbf{k}}^T}\,\frac{\Omega_{R,\mathbf{k}}^2}{\bar{\Gamma}_{\mathrm{cav},\mathbf{k}}^T + \bar{\Gamma}_{12,\mathbf{k}}}, \tag{71}$$

where we recall that $\bar{\Gamma}_{\mathrm{cav},\mathbf{k}}^T = \bar{\Gamma}_{\mathrm{cav},\mathbf{k}} + \bar{\Gamma}'_{\mathrm{cav},\mathbf{k}}$ is the total cavity broadening (due to the front and back mirror). In contrast, in the ultra-strong coupling regime, $\gamma_{\mathbf{k}}^{\mathrm{eff}}$ saturates around the value

$$\gamma_{\mathbf{k}}^{\mathrm{eff}} \simeq \frac{1}{2}\sqrt{\bar{\Gamma}_{\mathrm{cav},\mathbf{k}}^T \bar{\Gamma}_{12,\mathbf{k}}} \tag{72}$$

The numerical dependence of $\gamma_{\mathbf{k}}^{\mathrm{eff}}$ as a function of $\Omega_{R,\mathbf{k}}/\omega_{12}$ is shown in Fig. 7, showing the Purcell-like behavior (71) in the weak-coupling limit and the saturation value (72) in the very strong coupling limit. The slight decrease at large $\Omega_{R,\mathbf{k}}$ is due to the specific shape chosen for the real parts of the damping kernels $\Gamma_{\mathrm{cav},\mathbf{k}}(\omega)$ and $\Gamma_{12,\mathbf{k}}(\omega)$, which are constant for $\omega > 0$ and vanishing for $\omega < 0$, with a jump at $\omega = 0$. Due to the Kramers-Kronig relationship, the imaginary part (the Lamb shift) has a singularity at $\omega = 0$.

D. Comparison with free space case: enhancement of electroluminescence

It is interesting to compare the predictions for the ultra-strong coupling regime to what occurs for the isolated quantum well in the absence of the surrounding microcavity. In order for the comparison of the electroluminescence rates to be fair, exactly the same model (66) has to be used in both cases for the excitation of the intersubband transition by the electronic bath. A huge Hilbert space is in fact available for the electronic excitations of the present many-electron system, and the spontaneous emission rate dramatically depends on the specific state under consideration In our model, the only bright states are the ones created by the action of the electronic polarization field creation operators $b_{\mathbf{k}}^\dagger$, while the much larger number of other states remain dark. This is in stark contrast with what happens in a two-level atom, where the presence of a single excited state makes the spontaneous emission rate to be an univocally defined quantity. In particular, an explicit calculation of the quantum efficiency of the electroluminescence process with a realistic model of the electronic injection process would require a more refined model taking into account the energy that flows into all the dark excited states, orthogonal to the bright mode. For this reason, we do not attempt to estimate it in the present paper, but we rather focus our attention on comparing the predictions for the emission intensities that are obtained in the two cases using the very same model for the electronic injection mechanism.

In the absence of the surrounding microcavity, no coupling to any cavity mode is present, and the intersubband transition is directly coupled to free-space radiative modes. For the frequency-flat excitation of the electronic bath (66), the emission intensity can be analytically calculated to be:

$$\mathcal{L}_{\mathbf{k}}^{QW} = \rho_{\mathbf{k}}^{ph}\, I_{exc}^{el}\, \gamma_{\mathrm{bright},\mathbf{k}}^{QW}\,, \tag{73}$$

where $\gamma_{\mathrm{bright},\mathbf{k}}^{QW}$ is spontaneous emission rate of the bright intersubband excitation of wavevector $\mathbf{k}$ when the quantum well is embedded in a bulk material of refractive index ϵ_{QW} without any surrounding cavity.

For an electronic surface density in the quantum well equal to σ_{el}, the free-space spontaneous emission rate of the bright excitation mode is calculated by applying the Fermi's golden rule, giving the result

$$\gamma_{\mathrm{bright},\mathbf{k}}^{QW} = \frac{1}{2\sqrt{\epsilon_{QW}}}\,\frac{e^2}{c}\,\frac{N_{QW}\sigma_{el}}{2m_0}\,f_{12}\,\frac{\sin^2\theta}{\cos\theta} \tag{74}$$

where e is the electron charge, m_0 is the free electron mass, c the speed of light and N_{QW} the number of identical quantum wells. The propagation angle θ of the emitted photon is given by $\sin\theta = ck/(\omega_{12}\sqrt{\epsilon_{QW}})$. The oscillator strength f_{12} of the intersubband transition is written in terms of the electric dipole matrix element z_{12} as[32]:

$$f_{12} = \frac{2m_0\,\omega_{12}\,z_{12}^2}{\hbar}. \tag{75}$$

Note that the bright state $b_{\mathbf{k}}^\dagger\,|F\rangle$ is the excited state with the largest spontaneous emission rate. In particular, $\gamma_{\mathrm{bright},\mathbf{k}}^{QW}$ increases with the density of the two-dimensional electron gas and does not depend on the emission frequency ω_{12}. It is interesting to compare $\gamma_{\mathrm{bright},\mathbf{k}}^{QW}$ with the spontaneous emission rate of a different excited state of the two-dimensional

electron gas, namely $c^{(j)\dagger}_{2,\mathbf{k}+\mathbf{q}} c^{(j)}_{1,\mathbf{k}} |F\rangle$. In this case, the intersubband excitation does not coherently involve any longer all the electrons in the lower subband, but only the one initially at $\mathbf{k}$, so that the corresponding spontaneous emission rate is suppressed by a factor equal to the total number $N_{QW} N_{el}$ of electrons. Note that an atomic-like spontaneous emission rate[33] (i.e., proportional to $z_{12}^2 \omega_{12}^3$ and very weak for long wavelength transitions in the far infrared) is achieved only for a state like $c^{\dagger(j)}_{2,\mathbf{k}} |0_{cond}\rangle$ (one electron in the second subband, none in the first one). In contrast, the strong radiative properties of the bright state $b^\dagger_{\mathbf{k}} |F>$ with spontaneous emission rate $\gamma^{rad}_{\mathrm{bright},\mathbf{k}}$ occur in presence of a dense electron gas, as considered in this paper.

For a quantum well with very high barriers f_{12} does not depend on the quantum well thickness (i.e. on ω_{12}) and is approximately given by $f_{12} \simeq 0.96\, m_0/m^*$, m^* being the effective electronic mass in the semiconductor[23]. Using GaAs parameters ($\epsilon_{QW} = 13.5$, $f_{12} \simeq 14$), with an electron density $\sigma_{el} = 5 \cdot 10^{11}\,\mathrm{cm}^{-2}$ and $N_{QW} = 10$, the radiative linewith of the bright state is approximately $\hbar \gamma^{QW}_{\mathrm{bright},\mathbf{k}} \simeq 0.04\,\mathrm{meV}$.

Comparing this result with the one (72) for the ultra-strong coupling regime, the cavity-induced enhancement $\eta_{\mathbf{k}}$ of the spontaneous emission of the quantum well is given at resonance $\omega_{\mathbf{k}} = \omega_{12}$ by

$$\eta_{\mathbf{k}} \equiv \frac{\mathcal{L}_{\mathbf{k}}}{\mathcal{L}^{QW}_{\mathbf{k}}} = \frac{\gamma^{\mathrm{eff}}_{\mathbf{k}}}{\gamma^{QW}_{\mathrm{bright},\mathbf{k}}} \approx \frac{\sqrt{\bar{\Gamma}^T_{\mathrm{cav},\mathbf{k}} \bar{\Gamma}_{12,\mathbf{k}}}}{2\,\gamma^{rad}_{\mathrm{bright},\mathbf{k}}} \,. \tag{76}$$

For an intersubband transition for which $\hbar\omega_{12} \approx 100$ meV, typical values for the non-radiative broadening and the cavity mode broadening are $\hbar\Gamma_{12,\mathbf{k}}, \hbar\Gamma_{\mathrm{cav},\mathbf{k}} \approx 10\,\mathrm{meV}$. The enhancement is then as large as $\eta_{\mathbf{k}} \approx 100$.

The fact that (76) holds only in the strong coupling regime $\sqrt{\bar{\Gamma}^T_{\mathrm{cav},\mathbf{k}} \bar{\Gamma}_{12,\mathbf{k}}} \ll \Omega_{R,\mathbf{k}}$ imposes that:

$$\eta_{\mathbf{k}} \ll \frac{\Omega_{R,\mathbf{k}}}{\gamma^{rad}_{\mathrm{bright},\mathbf{k}}} \,, \tag{77}$$

which means that the enhancement can not made arbitrary large by simply choosing larger linewidths.

As a final remark, note that the expression (76) has been obtained under the resonant condition $\omega_{\mathrm{cav},\mathbf{k}} = \omega_{12}$ and is therefore expected to hold in a cone of wavevectors $\mathbf{k}$ around the resonant wavevector k_{res} such as $\omega_{\mathrm{cav},k_{res}} = \omega_{12}$. On the other hand, when the cavity mode resonance is detuned from the intersubband transition resonance of an amount larger than the linewidths, the enhancement with respect to free space case disappears.

VII. CONCLUSIONS AND PERSPECTIVES

In conclusion, we have presented a full quantum theory of cavities in the ultra-strong light-matter coupling regime (i.e. when the vacuum Rabi frequency is comparable to the active electronic transition frequency), including the coupling of the cavity system to dissipative baths. In the case of a time-independent cavity properties, we have solved exactly the quantum Langevin equations for the intracavity operators within an input-output approach and we have determined analytically the output operators, allowing us to determine the response of the cavity system to an arbitrary input.

In the case of a vacuum input for the photonic and electronic polarization fields, we have characterized the properties of the ground state of the cavity system: due to the anti-resonant terms of the light-matter interaction, it turns out to be a two-mode squeezed vacuum, whose properties are weakly renormalized by the interaction with the photonic and electronic baths. In particular, we have checked that the photons and electronic excitations present in the ground state are purely virtual ones, and can not escape from the cavity: if the input is in the vacuum state, the output is itself in the vacuum state and no radiation is emitted by the system. Furthermore, we have explicitly shown that if no anomalous correlations are present in the input beam, no correlations will be present in the output either, so that no extra-cavity squeezing is observable unless the input is itself squeezed.

On the other hand, the anomalous properties due to the antiresonant terms of the large vacuum Rabi coupling show up as a peculiar asymmetric anticrossing of the polariton excitation branches that can be easily observed in the optical reflection, transmission, and absorption spectra under coherent light excitation.

Finally, the input-output formalism has been applied to the study of the electroluminescence emission intensity in the case of an electronic excitation: the use of a microcavity surrounding the quantum well provides a significant enhancement of the emission performances as compared to the ones of an isolated quantum well.

As a future perspective, the theory presented here can be generalized to explore the interesting and fascinating scenario of a time-modulated cavity. Even in the case of a vacuum input for the photonic and electronic polarization fields, a non-adiabatic temporal variation of the vacuum Rabi frequency (which is possible in the case of intersubband

transitions in doped quantum well[7]) is expected to produce an output radiation of correlated photons[9], an effect reminiscent of the dynamical Casimir effect. The calculation of the quantum vacuum radiation spectra in the modulated case will be possible using and generalizing the comprehensive formalism developed in this paper.

Acknowledgments

We wish to thank A. Anappara, G. Bastard, V. Berger, Y. Castin, R. Colombelli, S. De Liberato, C. Fabre, L. Sapienza, C. Sirtori, A. Tredicucci, A. Vasanelli, A. Verger for discussions. LPA-ENS is a "Unité Mixte de Recherche Associé au CNRS (UMR 8551) et aux Universités Paris 6 et 7".

APPENDIX A: GENERALIZATION OF THE INPUT-OUTPUT THEORY INCLUDING ALSO THE ANTI-RESONANT COUPLING TERMS IN THE BATH HAMILTONIAN

In this Appendix, we generalize the input-output theory of the present system in order to include also the anti-resonant terms in the coupling with the photonic and electronic baths. These additional Hamiltonian terms make the calculations more cumbersome, but the results are still analytical. We have verified explicitly that when the broadening of the cavity and electronic transition modes is moderate, the effect of the anti-resonant terms in the bath Hamiltonians are negligible. The bath Hamiltonians including the antiresonant terms are

$$H_{bath}^{ph,gen} = H_{bath}^{ph} + i\hbar \int dq \sum_{\mathbf{k}} \left(\kappa_{q,\mathbf{k}}^{ph}\, \alpha_{q,\mathbf{k}}\; a_{\mathbf{k}} - \kappa_{q,\mathbf{k}}^{ph\,*}\, \alpha_{q,\mathbf{k}}^{\dagger} a_{\mathbf{k}}^{\dagger} \right) \ , \tag{A1}$$

and

$$H_{bath}^{el,gen} = H_{bath}^{el} + i\hbar \int dq \sum_{\mathbf{k}} \left(\kappa_{q,\mathbf{k}}^{el}\, \beta_{q,\mathbf{k}}\; b_{\mathbf{k}} - \kappa_{q,\mathbf{k}}^{el\,*}\, \beta_{q,\mathbf{k}}^{\dagger} b_{\mathbf{k}}^{\dagger} \right) \ , \tag{A2}$$

The generalized damping kernels

$$\gamma_{\mathrm{cav},\mathbf{k}}(t) = \Gamma_{\mathrm{cav},\mathbf{k}}(t) - \Gamma_{\mathrm{cav},-\mathbf{k}}^{\dagger}(t) \ , \tag{A3}$$

$$\gamma_{12,\mathbf{k}}(t) = \Gamma_{12,\mathbf{k}}(t) - \Gamma_{12,-\mathbf{k}}^{\dagger}(t) \ , \tag{A4}$$

and the generalized Langevin forces

$$f_{\mathrm{cav},\mathbf{k}}(t) = F_{\mathrm{cav},\mathbf{k}}(t) - F_{\mathrm{cav},-\mathbf{k}}^{\dagger}(t) \ , \tag{A5}$$

$$f_{12,\mathbf{k}}(t) = F_{12,\mathbf{k}}(t) - F_{12,-\mathbf{k}}^{\dagger}(t) \ . \tag{A6}$$

The quantum Langevin equations in frequency space become

$$\bar{\mathcal{M}}_{\mathbf{k},\omega}^{gen} \begin{pmatrix} \tilde{a}_{\mathbf{k}}(\omega) \\ \tilde{b}_{\mathbf{k}}(\omega) \\ \tilde{a}_{-\mathbf{k}}^{\dagger}(-\omega) \\ \tilde{b}_{-\mathbf{k}}^{\dagger}(-\omega) \end{pmatrix} + i \begin{pmatrix} \tilde{f}_{\mathrm{cav},\mathbf{k}}(\omega) \\ \tilde{f}_{12,\mathbf{k}}(\omega) \\ -\tilde{f}_{\mathrm{cav},\mathbf{k}}(\omega) \\ -\tilde{f}_{12,\mathbf{k}}(\omega) \end{pmatrix} = 0 \ , \tag{A7}$$

where

$$\bar{\mathcal{M}}_{\mathbf{k},\omega}^{gen} = \begin{pmatrix} \omega_{\mathrm{cav},k} + 2\bar{D}_k - \omega - i\tilde{\gamma}_{\mathrm{cav},\mathbf{k}}(\omega) & i\bar{\Omega}_{R,k} & 2\bar{D}_k - i\tilde{\gamma}_{\mathrm{cav},\mathbf{k}}(\omega) & -i\bar{\Omega}_{R,k} \\ -i\bar{\Omega}_{R,k} & \omega_{12} - \omega - i\tilde{\gamma}_{12,\mathbf{k}}(\omega) & -i\bar{\Omega}_{R,k} & -i\tilde{\gamma}_{12,\mathbf{k}}(\omega) \\ -2\bar{D}_k + i\tilde{\gamma}_{\mathrm{cav},\mathbf{k}}(\omega) & -i\bar{\Omega}_{R,k} & -\omega_{\mathrm{cav},k} - 2\bar{D}_k - \omega + i\tilde{\gamma}_{\mathrm{cav},\mathbf{k}}(\omega) & i\bar{\Omega}_{R,k} \\ -i\bar{\Omega}_{R,k} & i\tilde{\gamma}_{12,\mathbf{k}}(\omega) & -i\bar{\Omega}_{R,k} & -\omega_{12} - \omega + i\tilde{\gamma}_{12,\mathbf{k}}(\omega) \end{pmatrix} \tag{A8}$$

the output operators $\alpha^{out}_{q,\mathbf{k}}$ and $\beta^{out}_{q,\mathbf{k}}$ are related to the input and cavity ones by:

$$\alpha^{out}_{q,\mathbf{k}} = \alpha^{in}_{q,\mathbf{k}} - \kappa^{ph\star}_{q,\mathbf{k}}(\tilde{a}_{\mathbf{k}}(\omega^{ph}_{q,\mathbf{k}}) + \tilde{a}^{\dagger}_{-\mathbf{k}}(-\omega^{ph}_{q,\mathbf{k}})) \ , \tag{A9}$$

$$\beta^{out}_{q,\mathbf{k}} = \beta^{in}_{q,\mathbf{k}} - \kappa^{el\star}_{q,\mathbf{k}}(\tilde{b}_{\mathbf{k}}(\omega^{el}_{q,\mathbf{k}}) + \tilde{b}^{\dagger}_{-\mathbf{k}}(-\omega^{el}_{q,\mathbf{k}})) \ . \tag{A10}$$

As previously, Eq. (A7) can be solved exactly:

$$\begin{pmatrix} \tilde{a}_{\mathbf{k}}(\omega) \\ \tilde{b}_{\mathbf{k}}(\omega) \\ \tilde{a}^{\dagger}_{-\mathbf{k}}(-\omega) \\ \tilde{b}^{\dagger}_{-\mathbf{k}}(-\omega) \end{pmatrix} = \bar{\mathcal{G}}^{gen}(\mathbf{k},\omega) \begin{pmatrix} \tilde{f}_{\mathrm{cav},\mathbf{k}}(\omega) \\ \tilde{f}_{12,\mathbf{k}}(\omega) \\ -\tilde{f}_{\mathrm{cav},\mathbf{k}}(\omega) \\ -\tilde{f}_{12,\mathbf{k}}(\omega) \end{pmatrix} \ , \tag{A11}$$

where

$$\bar{\mathcal{G}}^{gen}(\mathbf{k},\omega) = -i \ [\bar{\mathcal{M}}^{gen}_{\mathbf{k},\omega}]^{-1} \ . \tag{A12}$$

The relation between the input and output operators is

$$\begin{pmatrix} \alpha^{out}_{q,\mathbf{k}} \\ \beta^{out}_{q',\mathbf{k}} \end{pmatrix} = \begin{pmatrix} \bar{\mathcal{U}}^{gen}_{11}(\mathbf{k},\omega) & \bar{\mathcal{U}}^{gen}_{12}(\mathbf{k},\omega) \\ \bar{\mathcal{U}}^{gen}_{21}(\mathbf{k},\omega) & \bar{\mathcal{U}}^{gen}_{22}(\mathbf{k},\omega) \end{pmatrix} \begin{pmatrix} \alpha^{in}_{q,\mathbf{k}} \\ \beta^{in}_{q',\mathbf{k}} \end{pmatrix} \ , \tag{A13}$$

with the generalized matrix

$$\bar{\mathcal{U}}^{gen}_{11}(\mathbf{k},\omega) = 1 - 2\Re\{\tilde{\Gamma}_{\mathrm{cav},\mathbf{k}}(\omega)\} \left[\bar{\mathcal{G}}^{gen}_{11}(\mathbf{k},\omega) + \bar{\mathcal{G}}^{gen}_{31}(\mathbf{k},\omega) - \bar{\mathcal{G}}^{gen}_{13}(\mathbf{k},\omega) - \bar{\mathcal{G}}^{gen}_{33}(\mathbf{k},\omega)\right] \ , \tag{A14}$$

$$\bar{\mathcal{U}}^{gen}_{12}(\mathbf{k},\omega) = -2\Re\{\tilde{\Gamma}_{12,\mathbf{k}}(\omega)\} \frac{\kappa^{ph\ \star}_{q,\mathbf{k}}}{\kappa^{el\ \star}_{q',\mathbf{k}}} \left[\bar{\mathcal{G}}^{gen}_{12}(\mathbf{k},\omega) + \bar{\mathcal{G}}^{gen}_{32}(\mathbf{k},\omega) - \bar{\mathcal{G}}^{gen}_{14}(\mathbf{k},\omega) - \bar{\mathcal{G}}^{gen}_{34}(\mathbf{k},\omega)\right] \ , \tag{A15}$$

$$\bar{\mathcal{U}}^{gen}_{21}(\mathbf{k},\omega) = -2\Re\{\tilde{\Gamma}_{\mathrm{cav},\mathbf{k}}(\omega)\} \frac{\kappa^{el\ \star}_{q',\mathbf{k}}}{\kappa^{ph\ \star}_{q,\mathbf{k}}} \left[\bar{\mathcal{G}}^{gen}_{21}(\mathbf{k},\omega) + \bar{\mathcal{G}}^{gen}_{41}(\mathbf{k},\omega) - \bar{\mathcal{G}}^{gen}_{23}(\mathbf{k},\omega) - \bar{\mathcal{G}}^{gen}_{43}(\mathbf{k},\omega)\right] \ , \tag{A16}$$

$$\bar{\mathcal{U}}^{gen}_{22}(\mathbf{k},\omega) = 1 - 2\Re\{\tilde{\Gamma}_{12,\mathbf{k}}(\omega)\} \left[\bar{\mathcal{G}}^{gen}_{22}(\mathbf{k},\omega) + \bar{\mathcal{G}}^{gen}_{42}(\mathbf{k},\omega) - \bar{\mathcal{G}}^{gen}_{24}(\mathbf{k},\omega) - \bar{\mathcal{G}}^{gen}_{44}(\mathbf{k},\omega)\right] \ . \tag{A17}$$

$$\tag{A18}$$

We have verified explicitly that the matrix $\bar{\mathcal{U}}^{gen}(\mathbf{k},\omega)$ is unitary. For the parameters used in this paper, $\bar{\mathcal{U}}^{gen}(\mathbf{k},\omega) \simeq \bar{\mathcal{U}}(\mathbf{k},\omega)$, where $\bar{\mathcal{U}}(\mathbf{k},\omega)$ is the unitary matrix (38-41) in the absence of the bath antiresonant terms.

---

* Electronic address: ciuti@lpa.ens.fr

[1] *Cavity quantum electrodynamics*, edited by P. R. Berman (Academic Press, Boston, 1994)
[2] J. M. Raimond, M. Brune, and S. Haroche, Rev. Mod. Phys. **73**, 565 (2001).
[3] C. Weisbuch , M. Nishioka, A. Ishikawa, Y. Arakawa, Phys. Rev. Lett. **69**, 3314 (1992).
[4] D. Dini, R. Kohler, A. Tredicucci, G. Biasol, and L. Sorba, Phys. Rev. Lett. **90**, 116401 (2003).
[5] A. Liu, Phys. Rev. B **55**, 7101 (1997).
[6] E. Dupont, H. C. Liu, A. J. SpringThorpe, W. Lai, and M. Extavour, Phys. Rev. B **68**, 245320 (2003).
[7] A. A. Anappara, A. Tredicucci, G. Biasiol, L. Sorba, Appl. Phys. Lett. **87**, 051105 (2005).
[8] R. Colombelli, C. Ciuti, Y. Chassagneux, C. Sirtori, Semicond. Sci. Technol. **20**, 985 (2005).
[9] C. Ciuti, G. Bastard, I. Carusotto, Phys. Rev. B **72**, 115303 (2005).
[10] C. W. Gardiner and M. J. Collett, Phys. Rev. A **31**, 3761 (1985).
[11] S. Reynaud and M. Heidmann, Opt. Comm. **71**, 209 (1989).
[12] D. F. Walls and G. J. Milburn, *Quantum Optics* (Springer-Verlag, Berlin, 1994).
[13] J. J. Hopfield, Phys. Rev. **112**, 1555 (1958).
[14] *Intersubband Transitions in Quantum Wells: Physics and Device Applications I*, edited by H. C. Liu and F. Capasso, Semiconductors and Semimetals Vol. 62 (Academic Press, San Diego, 2000).
[15] *Intersubband Transitions in Quantum Wells: Physics and Device Applications II*, edited by H. C. Liu and F. Capasso, Semiconductors and Semimetals Vol. 62 (Academic Press, San Diego, 2000).

[16] R. Ferreira and G. Bastard, Phys. Rev. B **40**, 1074 (1989).
[17] A. O. Caldeira and A. J. Leggett, Phys. Rev. Lett. **46**, 211 (1981).
[18] This kind of effective bath for the electronic degrees of freedom has been considered in the case of excitonic transitions by J. Ph. Karr, A. Baas, and E. Giacobino, Phys. Rev. A **69**, 063807 (2004).
[19] For the Fourier transforms, we have used the definition $\tilde{A}(\omega) \equiv \mathcal{F}[A(t)](\omega) \equiv \int_{-\infty}^{\infty} dt\ e^{i\omega t} A(t)$. For the Fourier transforms of hermitian conjugated operators, we will use the simplified notation $\tilde{A}^{\dagger}(-\omega) \equiv \mathcal{F}[A^{\dagger}(t)](\omega) \equiv (\tilde{A}(-\omega))^{\dagger}$.
[20] C. Cohen-Tannoudji, J. Dupont-Roc, and G. Grynberg, *Atom-Photon Interactions. Basic Processes and Applications.*, (Wiley Science Paperback Series, New York, 1998).
[21] F. Bloch and A. Siegert, Phys. Rev. **57**, 522 (1940)
[22] J. Zakrzewski, M. Lewenstein, and T. W. Mossberg, Phys. Rev. A **44**, 7717 (1991); *ibidem* **44**, 7732 (1991); *ibidem* **44**, 7746 (1991).
[23] G. Bastard, *Wave Mechanics Applied to Semiconductor Heterostructures* (Halsted Press, New York, 1988).
[24] G. T. Moore, J. Math. Phys. (N.Y.) **11**, 2679 (1970); S. A. Fulling and P. C. W. Davies, Proc. R. Soc. London A **348**, 393 (1976); M. Kardar and R. Golestanian, Rev. Mod. Phys. **71**, 1233 (1999).
[25] For a recent review, see A. Lambrecht, J. Opt. B: Quantum Semiclass. Opt. **7**, S3 (2005).
[26] S. De Liberato, C. Ciuti, I. Carusotto, in preparation.
[27] M. Artoni and J. L. Birman, Phys. Rev. B **44**, 3736 (1991).
[28] P. Schwendimann and A. Quattropani, Europhys. Lett. **17**, 355 (1992).
[29] Z. Hradil, A. Quattropani, V. Savona, and P. Schwendimann, Journ. of Stat. Phys. **76**, 299 (1994).
[30] E. M. Purcell, Phys. Rev. **69**, 681 (1946).
[31] J. M. Gérard, B. Sermage, B. Gayral, B. Legrand, E. Costard, and V. Thierry-Mieg, Phys. Rev. Lett. **81**, 1110 (1998).
[32] C. Sirtori, F. Capasso, J. Faist, S. Scandolo, Phys. Rev. B **50**, 8663 (1994).
[33] E. Rosencher, B. Vinter, *Optoelectronics*, (Cambridge University Press, Cambridge, UK, 2002).
[34] Note that the anti-resonant terms H_{anti} in the Hamiltonian are due to the same *vacuum* Rabi coupling responsible for the resonant terms H_{res}. Hence, this problem, although there is some formal reminiscence, is different from the case of antiresonant transitions and Bloch-Siegert-like shifts[21] induced by a *classical* Rabi coupling produced by an intense and coherent pump field, which is comprehensively studied in Ref.22.